Hydrogen line observations: From frugal to advanced
Part 1: Introduction and antenna options

Wolfgang Herrmann and the Astropeiler "Hydrogen Team"

1. Introduction

Observing the emission of neutral hydrogen from our galaxy has become a very achievable target for amateurs. Low cost components have become readily available over the recent years which substantially facilitate the observation possibilities. There are quite a few options to approach hydrogen observations, varying in technical and financial effort. Achievable results will be different depending on such effort, but as will be demonstrated some basic observations are possible with a very frugal approach.

The whole subject will be presented in a series of articles intending to give an overview of various options and to do a comparison between these. Each component of a receiving chain will be dealt with one by one: The antenna, the low noise amplifier, filter and the receiver itself (the "backend" in radio astronomy parlance). Once the individual components are covered, a comparison between various setups using these components is done. Actual observations are performed in order to allow an apples to apples comparison to the extent possible.
Hopefully this series will be encouragement to try hydrogen line observations and give guidance to those who want to give it a try.

This first part of the series will look at the Physics behind this emission, the history of its discovery and deal with various options for antennas.

2. What is the hydrogen line emission?

The Dutch astronomer H.C. van de Hulst predicted the existence of an emission line from hydrogen in the interstellar space back in 1945 [1]. This emission originates from a transition between the hyperfine structure levels in the 1s electronic ground state of the hydrogen atom, which differ by the spin orientation of the proton and the electron (fig. 1):
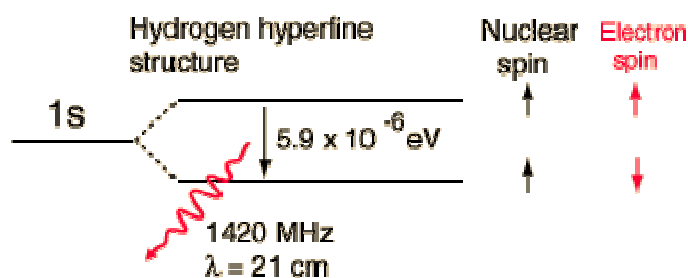

Figure 1: Hyperfine structure transition of hydrogen
Graphic from [2]

The small energy difference between the two states corresponds to a photon of 21 cm wavelength or a frequency of about 1420 MHz.

The excitation of this line is believed to be caused by collisions between the hydrogen atoms in the interstellar space. The collision energy (or parts thereof) is transferred into the atom and then released as electromagnetic radiation as the hydrogen atom transits from the excited state to the energetically lower state.

It is quite amazing when one looks at the numbers which govern this process: The probability of one hydrogen atom colliding with another one in the interstellar space is about once per 60 years. The lifetime of the transition is about 11 million years which means it takes an average of 11 million years after the excitation before the energy is released again in form of electromagnetic radiation. Therefore, the hydrogen emission line is very faint. It is only because we are observing very large volumes that we are able to receive a signal.

3. First hydrogen line observations and current surveys

Even though v.d. Hulst predicted the line theoretically, he was quite sceptical about the possibility of actually observing it. Nevertheless, the line was finally detected by Ewen and Purcell in March 1951 [3] and shortly thereafter by Muller and Oort [4].

It is interesting to read the story behind the detection provided by "Doc" Ewen at the NRAO archive website [5]. A lot of details are given about the setup in the slides provided at this site.

Ewen and Purcell used a frequency switching technique to overcome the variations in the spectral response of their instrument. Due to this technique, the observed line is shown twice, both positive and negative as shown in one of their recordings (fig. 2).
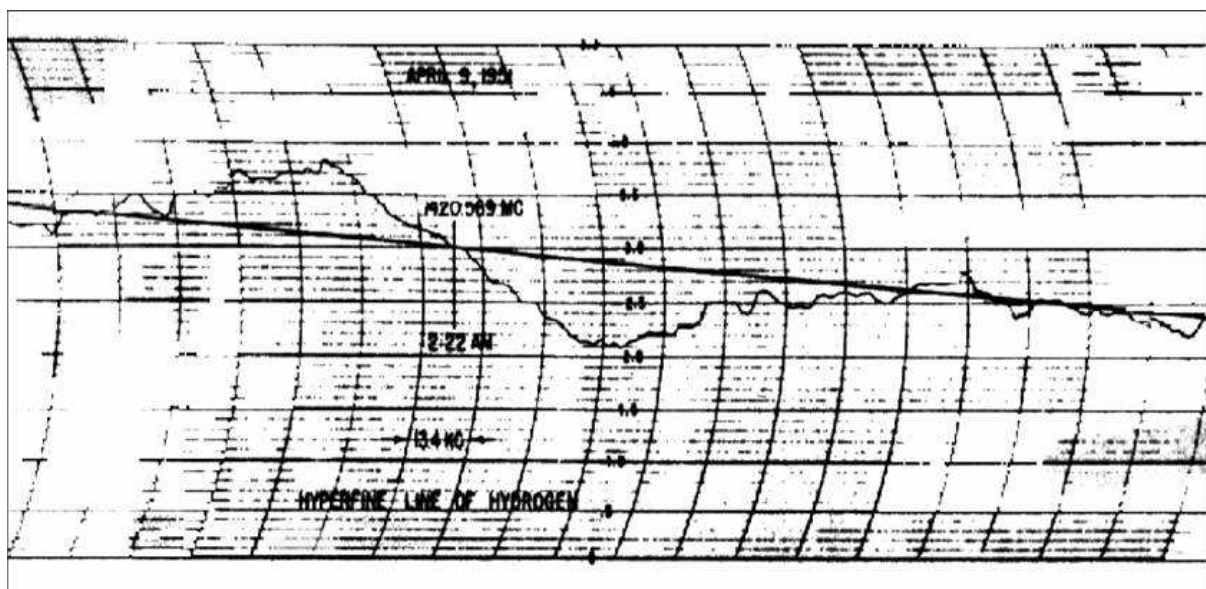

Figure 2: Early recording of the hydrogen line
Reproduced from [5]

They used a horn antenna as shown in fig. 3. The aperture of the horn was 109 cm x 142 cm [5]. The noise figure of their receiver was 11 dB [3].

Figure 3: Ewen pictured with his horn
From [6]

The Dutch group had a larger aperture, using a 7.5 m dish. They reported a noise figure for the total receiving chain of 13 dB, and a frequency switching method was used as well.

These famous detections started a large amount of research activities, and surveys of the neutral hydrogen emission at 21cm are an ongoing effort even today.

The most recent full sky survey has been performed with the Effelsberg and Parkes telescopes, the HI4PI survey [7]. This work has delivered high resolution data which is made publicly available through the CDS Strasbourg data centre [8].

4. Distribution of hydrogen and Doppler shift

From all these surveys a very detailed picture of the hydrogen distribution in our galaxy is available. A representation from the HI4PI survey is depicted in fig. 4. It shows the density of hydrogen in galactic coordinates in Hammer Aitoff projection. As one can see, the highest density is in the galactic plane whereas lower density hydrogen clouds can be found almost all over the sky.
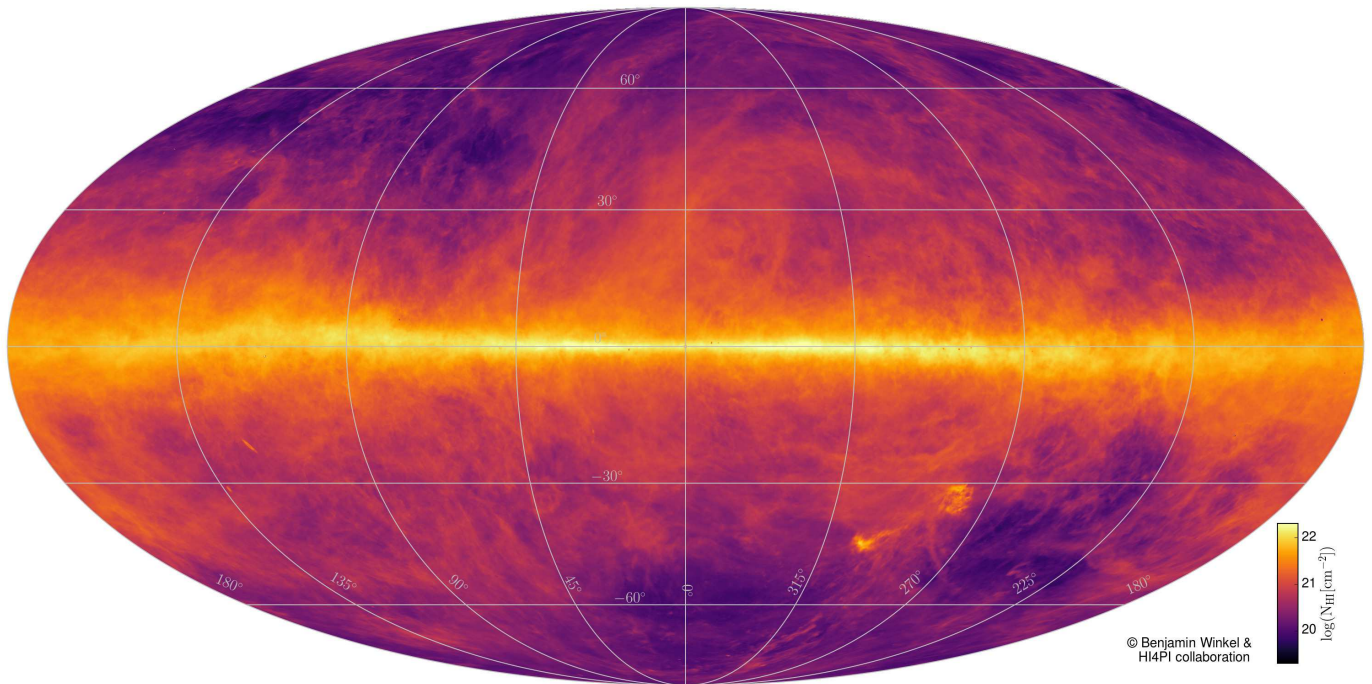
Figure 4: Hydrogen Density in Galacitc Coordinates
Source: Benjamin Winkel and the HI4PI Collaboration [9]

However, not only the hydrogen density can be determined by observing it's emission. Since it is a spectral line, Doppler shifts can be observed. Such shifts occur due to the motion of various hydrogen clouds within our galaxy.
The observations of these Doppler shifts have been instrumental in determining the inner structure of the Milky Way. This was recognized by the Dutch astronomers Oort, Kerr and Westerhout and published in their paper from 1958 [10].

The variation of velocity based on the HI4PI data has been nicely demonstrated in a video animation provided by Benjamin Winkel. It is a "must see" for all "hydrogen aficionados" [11]. Another way of representing the hydrogen Doppler shifts is to convert it to audio. We ourselves have prepared such a demonstration of the Doppler shift based on data recorded with our 25 m dish covering the galactic plane as a Youtube video [12].

5. What is in for the amateur?

Now with all these nice and shiny pictures and videos created from large dish data, what can one do with a much more modest setup available for amateurs?

A first indication can already be found by looking at Ewen's horn and instrumentation. The horn is of a moderate size and may be well within the reach of an ambitious

amateur. Looking at his instrumentation data one finds that his receiver has a very high noise figure by today's standards. This is at least an order of magnitude higher than what can be achieved these days.

From this one can conclude that observing the hydrogen emission may be a very reachable target for the amateur. In fact, there have been numerous successful observations by amateurs with various types of instruments.

6. Basic setup of a hydrogen line receiving system

A very generic picture of a setup to observe hydrogen is shown in fig. 5:
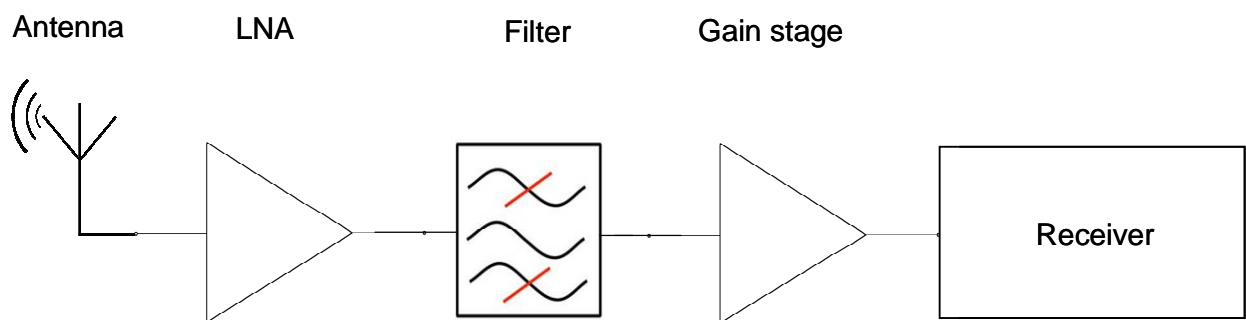

Figure 5: Generic setup

Obviously, the starting point is an antenna which is followed by a low noise amplifier (LNA). In order to suppress interference from terrestrial transmitters a filter is likely to be required. A couple of considerations will determine what kind of filter (if any) will be needed:
- Local radio frequency interference (RFI) environment
- Frequency selectivity of the antenna itself
- Capability of the receiver to handle strong signals adjacent to the receiving frequency

Depending on the gain of the LNA and the sensitivity of the receiver a further gain stage is likely to be required between the filter and the receiver. The receiver itself needs to have the capability to provide the frequency resolution as required by the hydrogen line, and of course needs to support a receiving frequency in the range of 1420 MHz.

In this series of articles we will walk through the various parts of the setup and see what options are available for each of them.

7. Antenna options

We have investigated and characterized a large number of antennas of very different design. Even though some of them seem to be very simple, all of them have in common that we were able to observe the hydrogen emission using these antennas. The results of these observations will be reported in a subsequent article of this series. Here we start describing the design and characteristics of the antennas themselves.

7.1. Methods for characterization

For most of these antennas we have measured the return loss. This is an indication on how well the antenna is resonant at 1420 MHz and how well the impedance is matched between the antenna and a LNA at 50 Ohms.

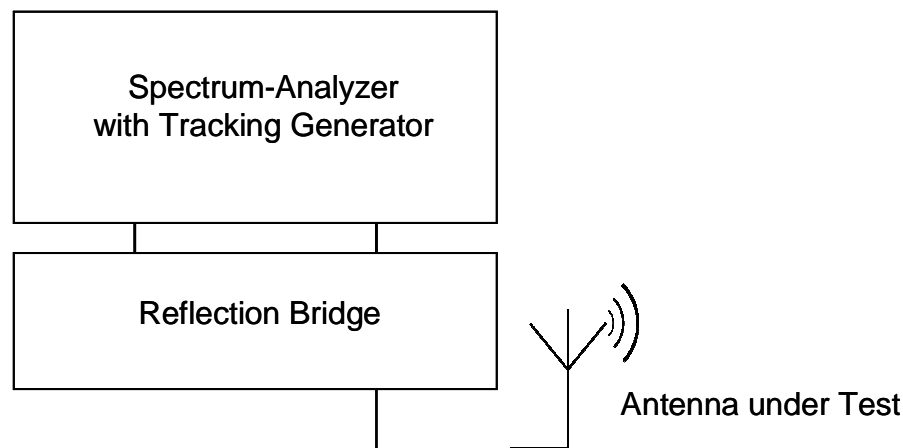The setup for this measurement is shown below in fig. 6

Figure 6: Antenna return loss measurement setup

A Siglent SSA 3000X spectrum analyzer with built in tracking generator was used in conjunction with a Siglent RBSSA3X20 reflection bridge for these tests.

For a few selected antennas we have also measured the pattern of the antennas. We have used a setup where a signal was generated by a signal generator (0 dBm) and transmitted by a log-periodic antenna. At a distance of about 35 m the antenna to be tested was mounted in a way that it could be rotated by 180°. A MPU9150 sensor was attached to the antenna mount which provided the information of the orientation of the antenna. A spectrum analyzer was used to measure the received power. Both the MPU sensor and the spectrum analyzer were connected to a Raspberry Pi computer which read both the orientation and the received power and continuously recorded the readings.
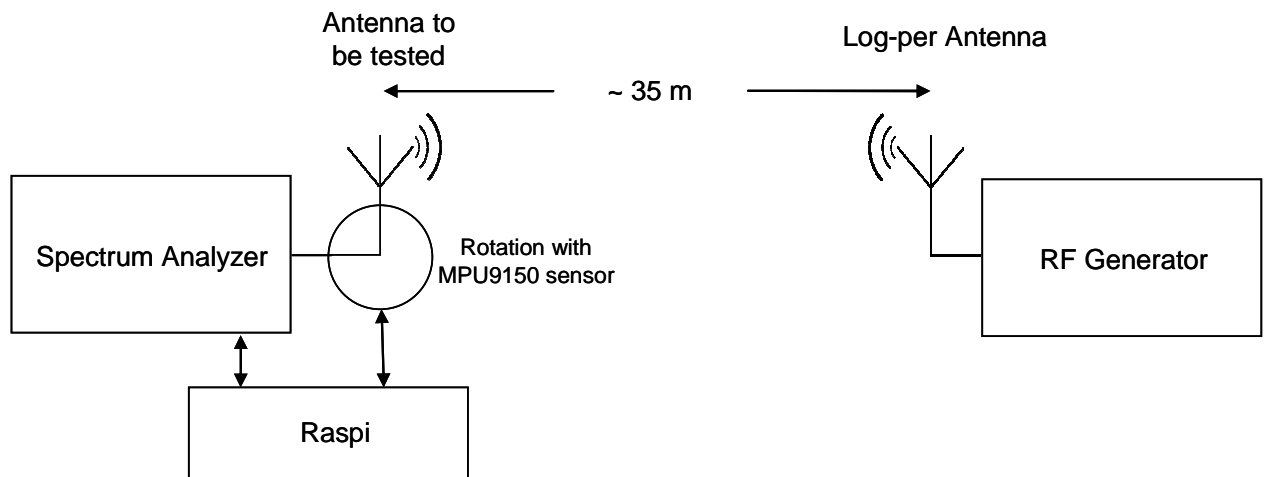
The setup is shown in fig. 7. below

Figure 7: Setup for antenna pattern measurement

Figure 8: Photos of setup (left receive side with one of the antennas tested, right transmit side)

The photos in fig. 8 show the practical setup. The small blue board on the white breadboard attached to the antenna fixture contains the MPU 9150 sensor.

Of course this setup cannot compete with a professional environment in an anechoic chamber. However care was taken that the natural foliage provided a reasonable absorption environment to at least avoid reflection as much as possible.

The measurement was taken in two orientations by flipping both receive and transmit antennas by 90°. Care was taken that the polarizations of both antennas were aligned.

A very rough calibration of the absolute antenna gain could be obtained by comparing the received signal from the antennas with a simple dipole. This was under the assumption that the dipole did achieve the theoretical gain known for dipoles. Since the dipole will not have been perfect, the gain values determined should therefore be taken with some caution.

7.2. Dipole antenna with balun
7.2.1. Design
This is probably the simplest antenna one can think of: A dipole antenna with a balun to adapt the symmetrical structure to the coaxial input of a LNA.
We have followed the design proposed by Matjaž Vidmar in [13]. There he describes how a dipole with a balun can be easily made from semi rigid cable. In the Matjaž paper such a dipole is used to excite a short backfire antenna. We have just used the dipole, adjusting the dimensions given in the paper to the wavelength of 21cm.
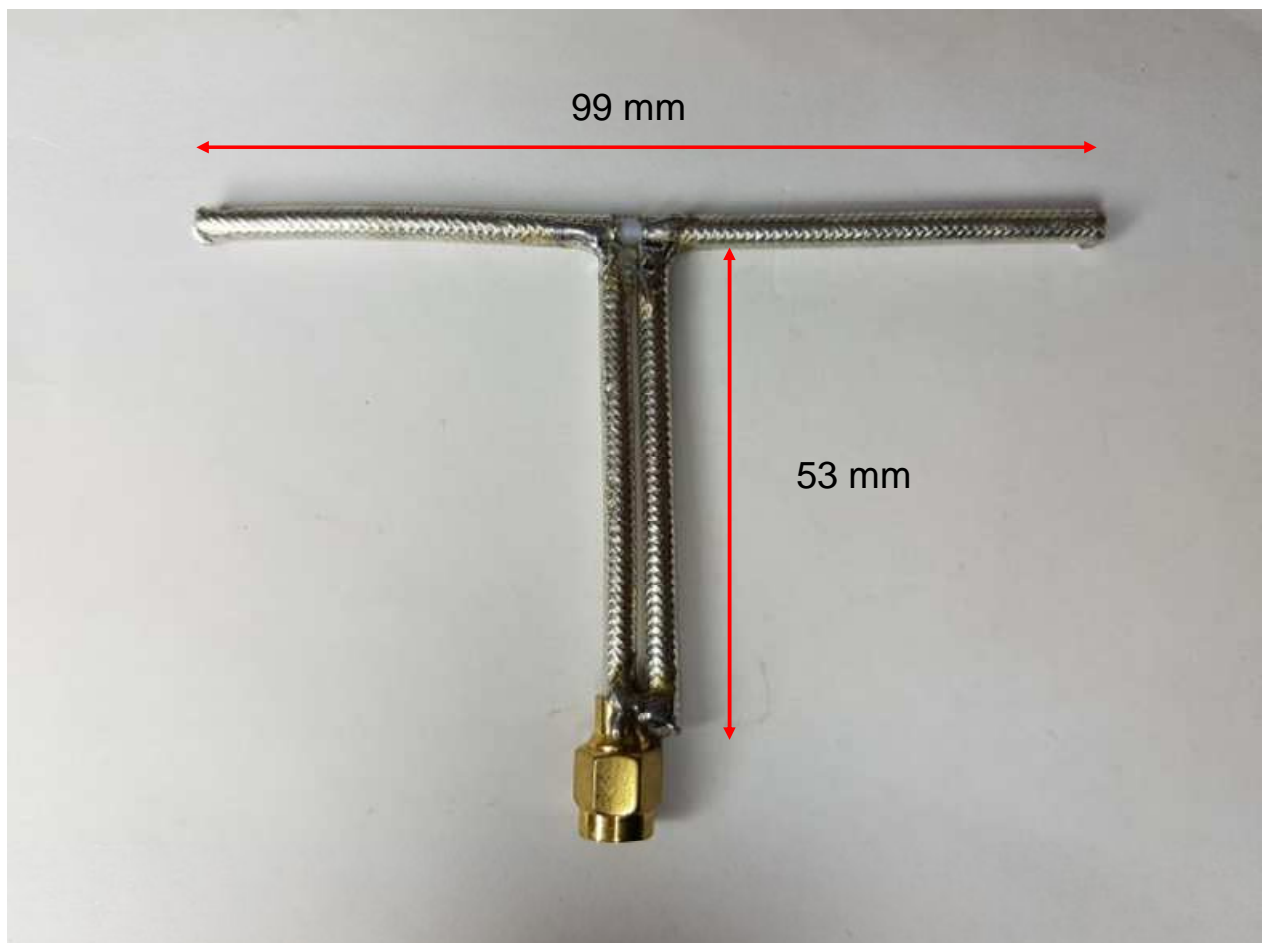The result is shown in fig. 9.

Figure 9: Dipole antenna

The dipole itself was made from a piece of semi rigid cable where the outer conductor was removed in the middle for ~2 mm. The inner conductor was connected to the outer conductor at each end. Another piece of semi rigid cable was fitted with a SMA connector at one end. At the other end, the outer conductor was soldered to the outer conductor of one of the dipole halves. The inner conductor was connected to the outer conductor of a third piece of semi rigid cable. This piece is soldered at one end to the outer conductor of the second half of the dipole and to the outside of the SMA cable at the other end.

An air gap is maintained between the two vertical cable pieces. As a picture says more than thousand words, please see fig. 10 below on how things are connected.
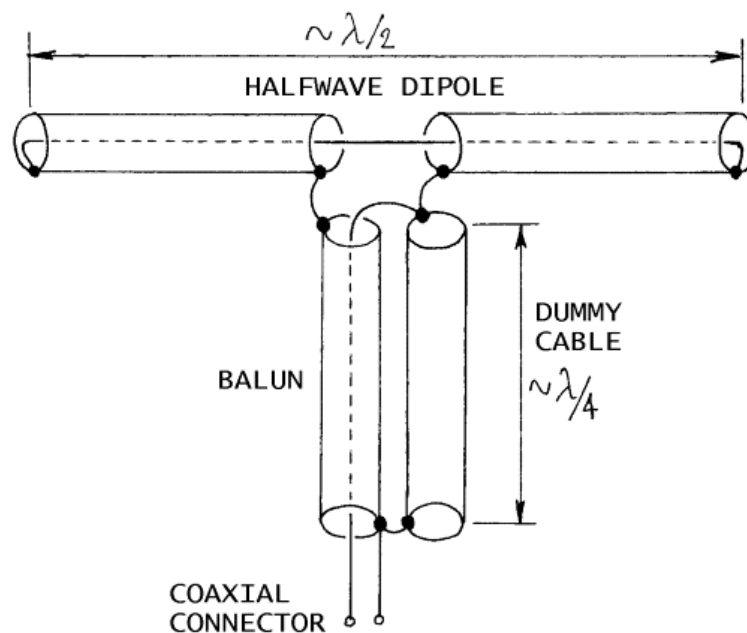

Figure 10: Dipole antenna electrical connections
Drawing from [13]

7.2.2. Characteristics

The return loss of the antenna is 10.7 dB at 1420 MHz with a relatively wide resonance curve as shown in fig. 11.
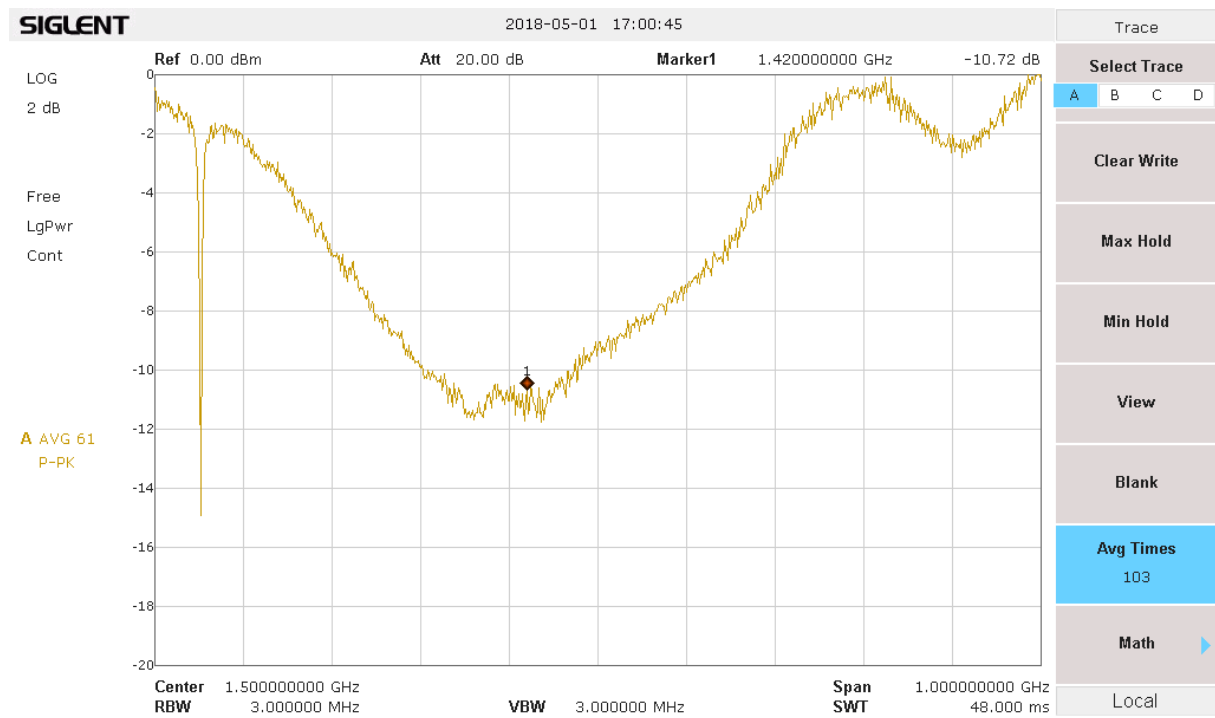
Ref 0.00 dBm   Att 20.00 dB   Marker1   1.420000000 GHz   -10.72 dB

LOG
2 dB

Free
LgPwr
Cont

A AVG 61
P-PK

0
-2
-4
-6
-8
-10
-12
-14
-16
-18
-20

1

Center 1.500000000 GHz
RBW 3.000000 MHz
VBW 3.000000 MHz
Span 1.000000000 GHz
SWT 48.000 ms

Select Trace
A B C D

Clear Write

Max Hold

Min Hold

View

Blank

Avg Times
103

Math ▶

Local

Figure 11: Dipole return loss measurement

7.3. Dipole with reflector

7.3.1. Design

A variant of the previous antenna can be built by adding a reflector. We have simply used a CD where the metallisation represents the reflecting surface.

We found that in this case the dipole needs to be a bit shorter in order to be resonant at 1420 MHz. A length of 89 mm was chosen instead of 99 mm. The balun is unchanged. The reflector is positioned at half the balun length and glued in place, see fig. 13:

Figure 12: Dipole with CD as reflector

7.3.2. Characteristics

The return loss of the antenna is 19.9 dB at 1420 MHz. Compared to the dipole without reflector the resonance is much sharper as shown in fig. 14.
For a simple dipole the expected gain is 2.1 dBi. Compared to this, the gain for this antenna has been measured to be 5 to 7 dBi, see fig. 15.
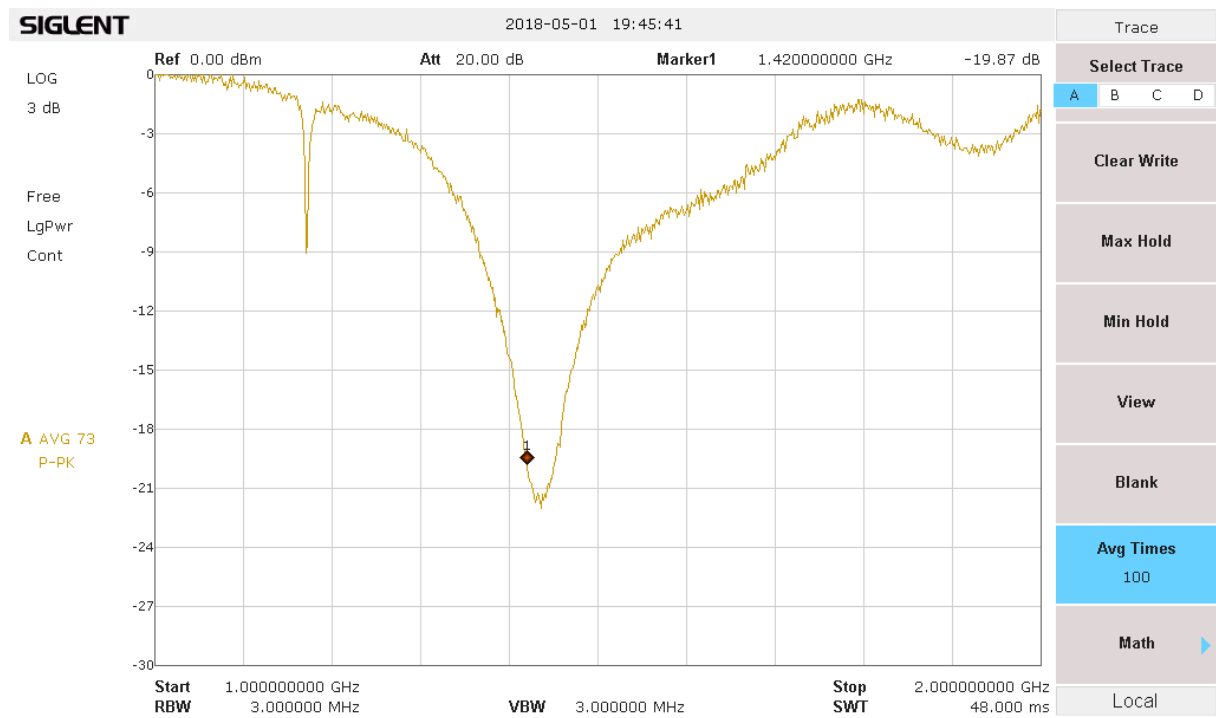
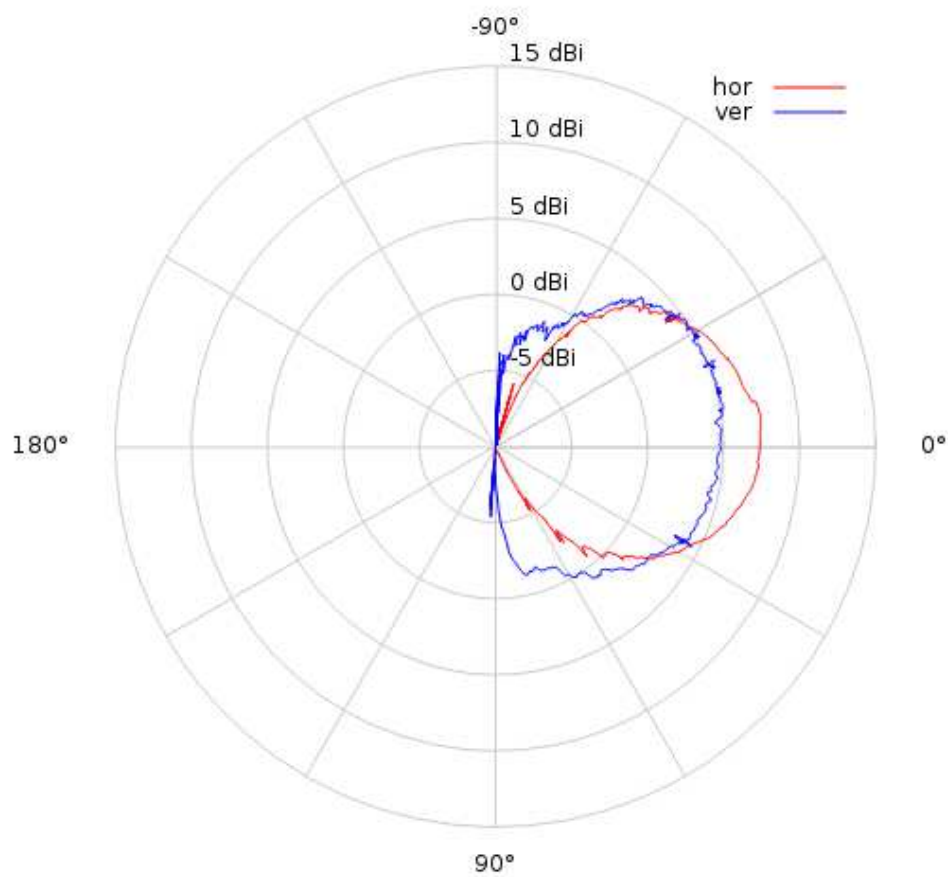**Figure 13: Dipole with reflector return loss measurement**

Figure 14: Dipole with reflector antenna pattern

7.4. Dipole with reflector, variant
7.4.1. Design
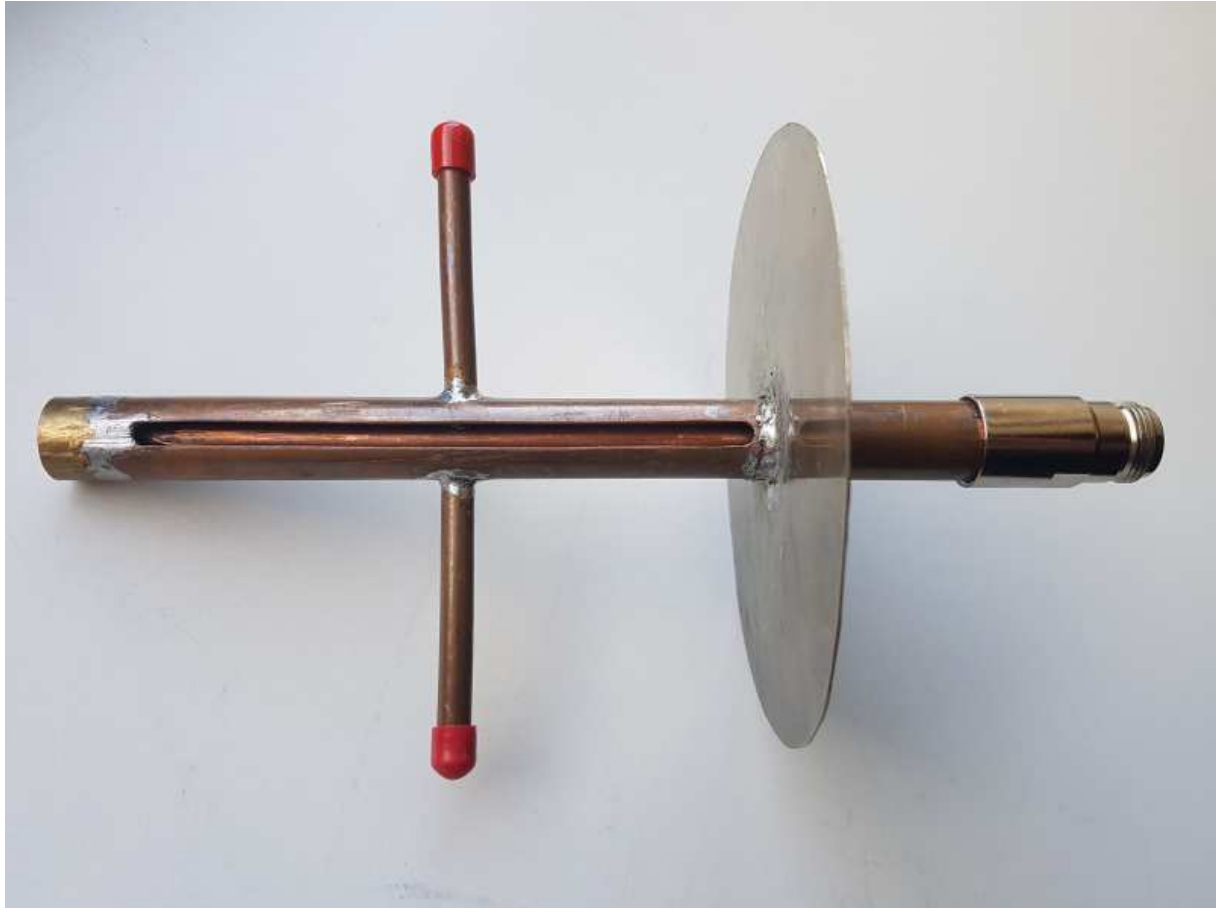This is another variant of a dipole with reflector shown in fig. 16.

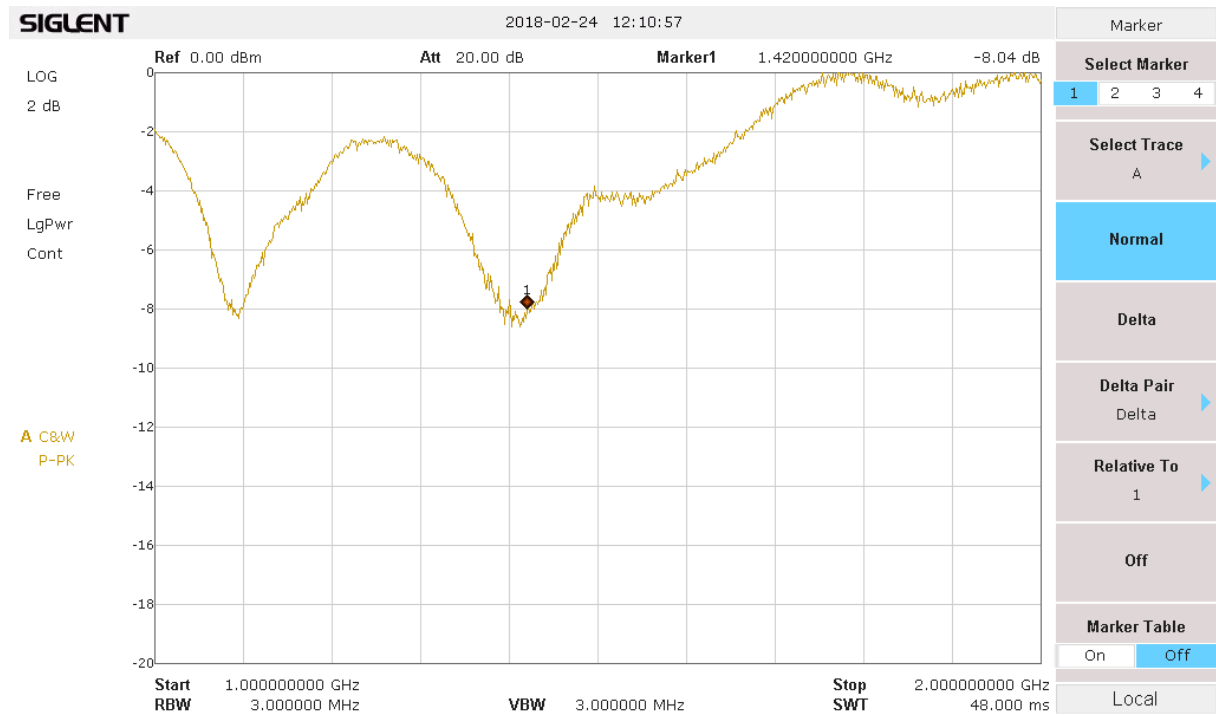**Figure 15: Dipole with reflector, variant**

7.4.2. Characteristics

Figure 16: Dipole with reflector (variant) return loss measurement

Compared to the other dipole with reflector, this design has less return loss and the resonance seem to be less sharp (fig. 16).

7.5. Circular waveguide (aka "stove pipe")

7.5.1. Design

A very easy to make design is a circular waveguide. This is also frequently used as a feed antenna for parabolic dishes and made from all sorts of cans. Therefore it is sometimes called a "cantenna". In our case we have used a stove pipe which is sold in hardware stores. For such stove pipes also end caps are available which makes it easy to have a reflecting end. The only thing which remains to be done is to drill a hole for a probe and mount this probe using a flange N-connector. In our case the stove pipe has a diameter of 15 cm and a length of 45 cm. The probe is placed at 9.3 cm from the reflecting end, see fig. 17.
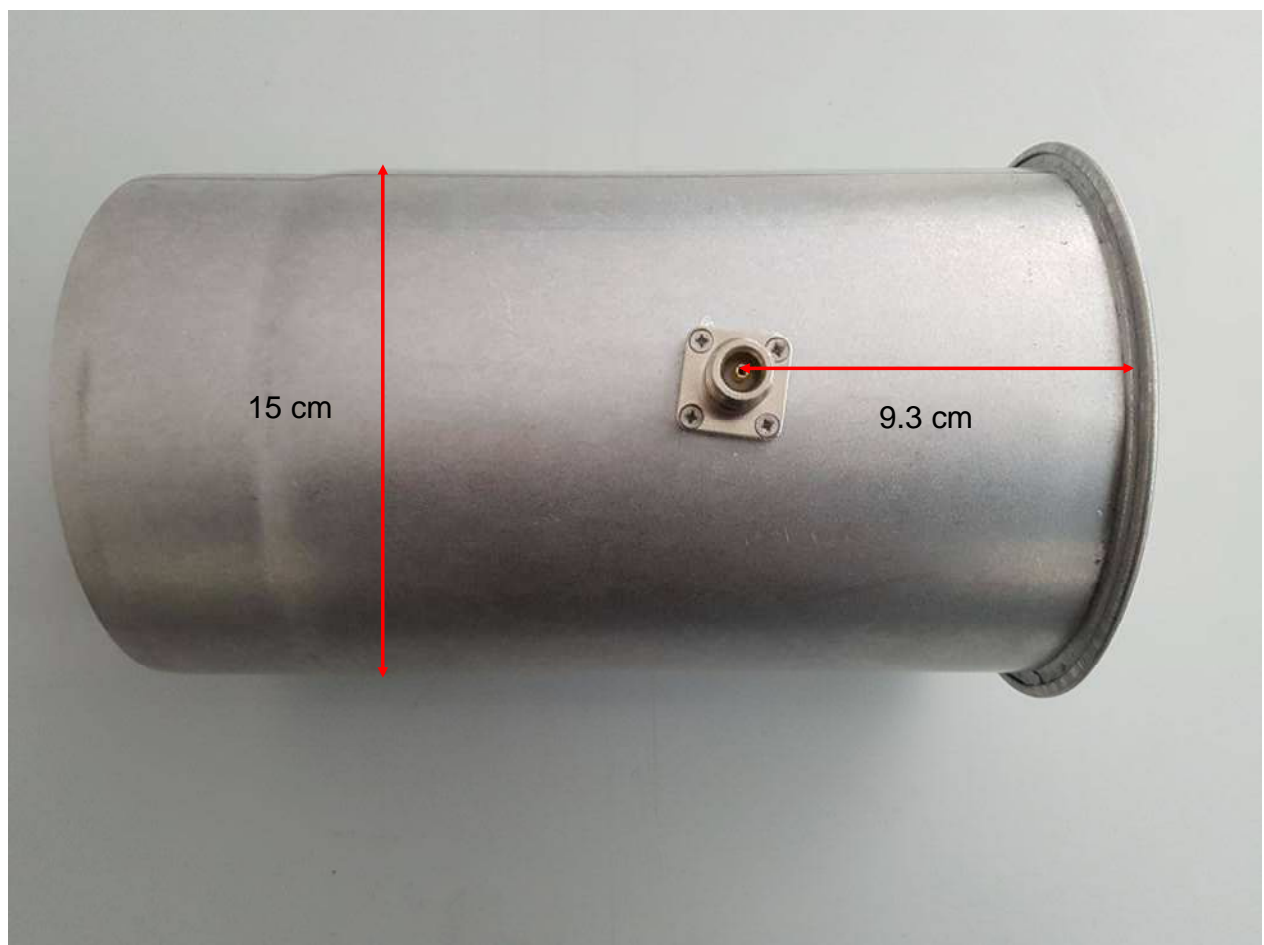

Figure 17: "Oven pipe" circular waveguide

This distance is a quarter wavelength of the waveguide wavelength. Please note that the wavelength inside the waveguide is longer than the wavelength in free space and depends on the diameter. The waveguide wavelength in a circular waveguide can be calculated as follows:

$$\lambda_G = \frac{\lambda}{\sqrt{1 - \frac{\lambda^2}{2.910\,D^2}}} \quad (1)$$

where λ_G is the guide wavelength, λ is the free space wavelength and D is the diameter of the waveguide-

The length of the pipe is not critical, it just needs to be longer than 3/4 of the guide wavelength. The probe should theoretically have a length of 1/4 of the free space wavelength which would be 5.25 cm. We found, however, that the return loss is improved at a length of 4.9 cm (fig. 18).
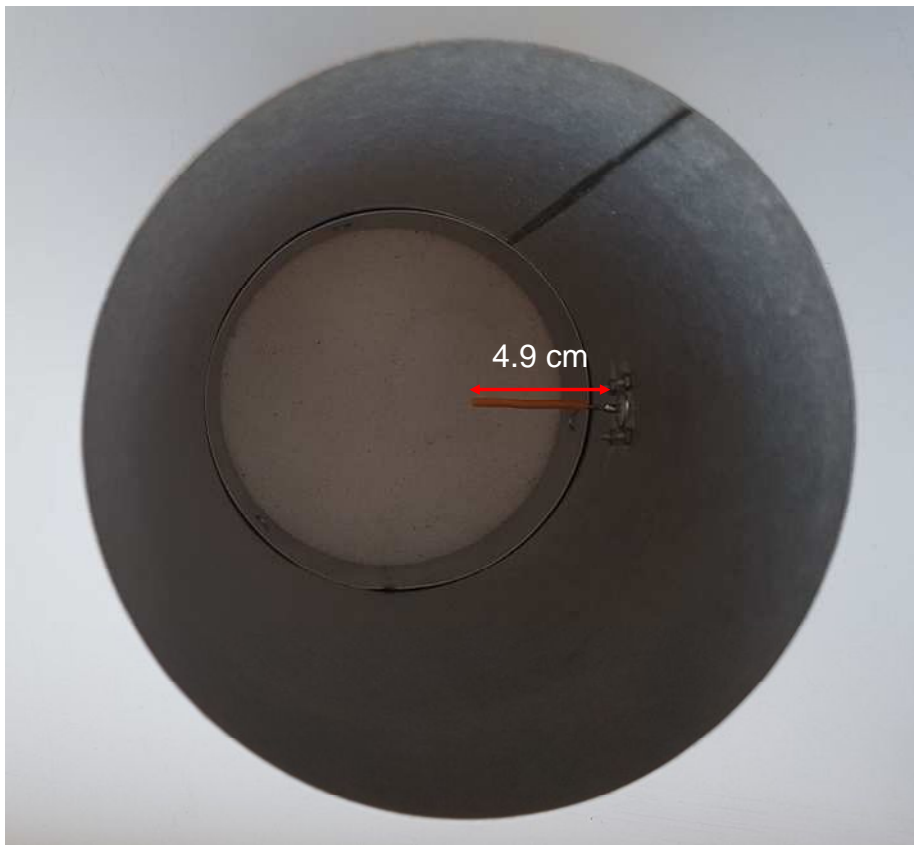

Figure 18: "Stove pipe" circular waveguide inside
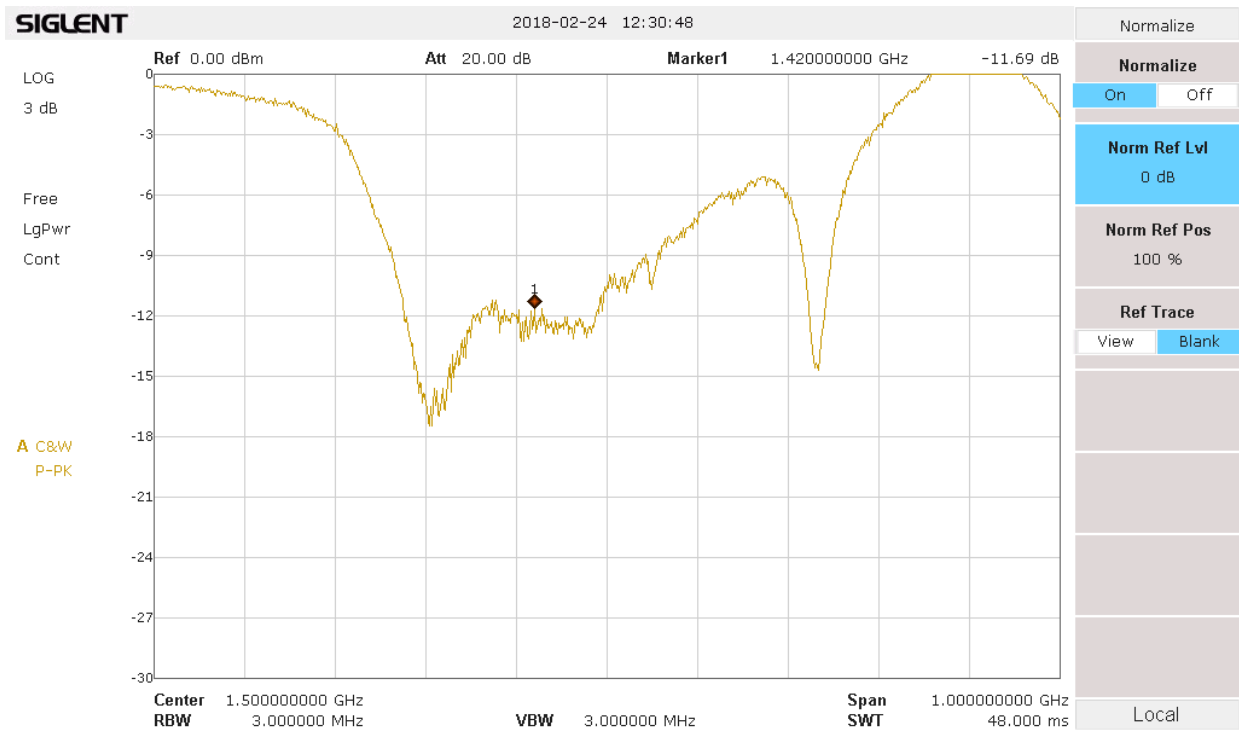
7.5.2. Characteristics

Figure 19: Circular Waveguide Return Loss

As expected, the return loss (11.6 at 1420 MHz) is fairly constant over a certain frequency range (fig. 19).

7.6. L-band rectangular waveguide
7.6.1. Design
This is simply a L-band waveguide with a probe with an N-Connector. It is a commercial product which we had in storage (fig. 20) with a WG 6 flange.

Figure 20: Rectangular Wave Guide

7.6.2. Characteristics

The return loss is greater than 10 dB over a large range (fig. 21), and therefore it should be usable over a wide frequency range. At 1420 MHz the return loss is 13.8 dB.

The wide frequency range is probably a result of the large size of the probe. The disadvantage of this wide frequency range might be that a lot of RFI can be picked up.
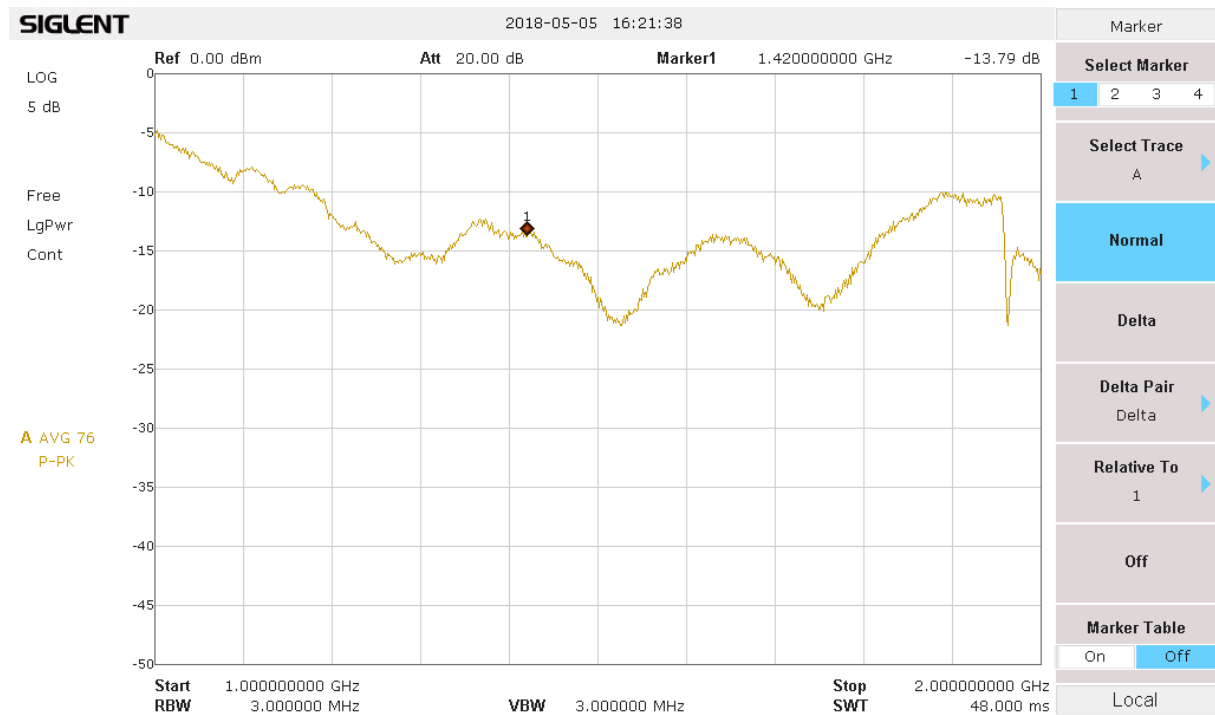

Figure 21: L-band Rectangular Waveguide Return Loss

7.7. Home brew L-Band rectangular waveguide (aka Crazy Box)
7.7.1. Design

Admittedly this is a somewhat strange design and was basically created for the fun of doing it. It is a wooden box covered with aluminium foil (fig. 22). An N-connector was placed at a quarter of the waveguide wavelength holding a wire as a probe. This is essentially a rectangular wave guide similar to the one above.

The dimensions are 15 cm width, 10 cm height and 21 cm depth. The probe is placed at 7 cm from the rear reflecting surface which is a bit closer than the theoretical guide quarter wavelength which would be 7.4 cm.

Figure 22: Wooden box waveguide

7.7.2. Characteristics

To our great surprise this box had a fairly good return loss of almost 20 dB at 1420 MHz as shown in fig. 23. The comparatively good return loss, however, could also be due to the lossy nature of this assembly.
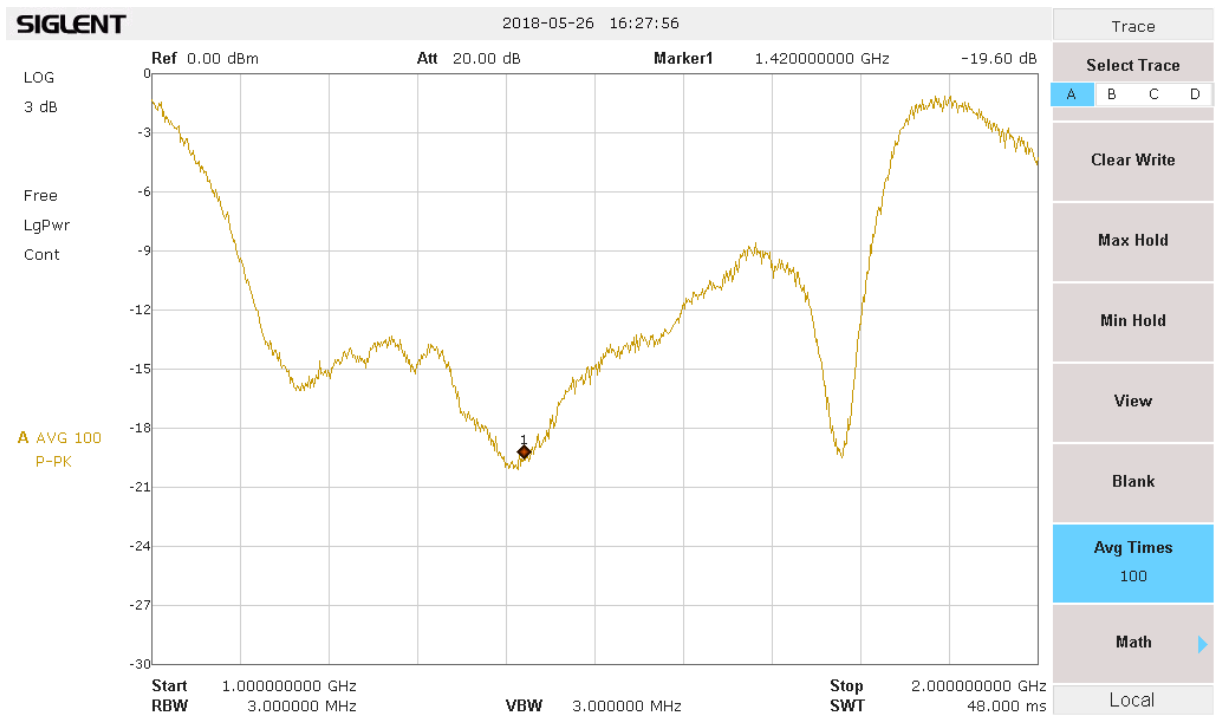

Figure 23: Wooden Box Waveguide Return Loss

7.8. Air gap patch antenna

7.8.1. Design

The air gap patch antenna consists of a quadratic radiator mounted on top of a quadratic reflector. Both metal planes are separated by a gap (the "air gap") which in this case is 7.5 mm. They are connected to each other in the middle. The connection is conductive. The radiator is excited at a position 26 mm from the side. Fig. 24 shows a top view of the antenna.
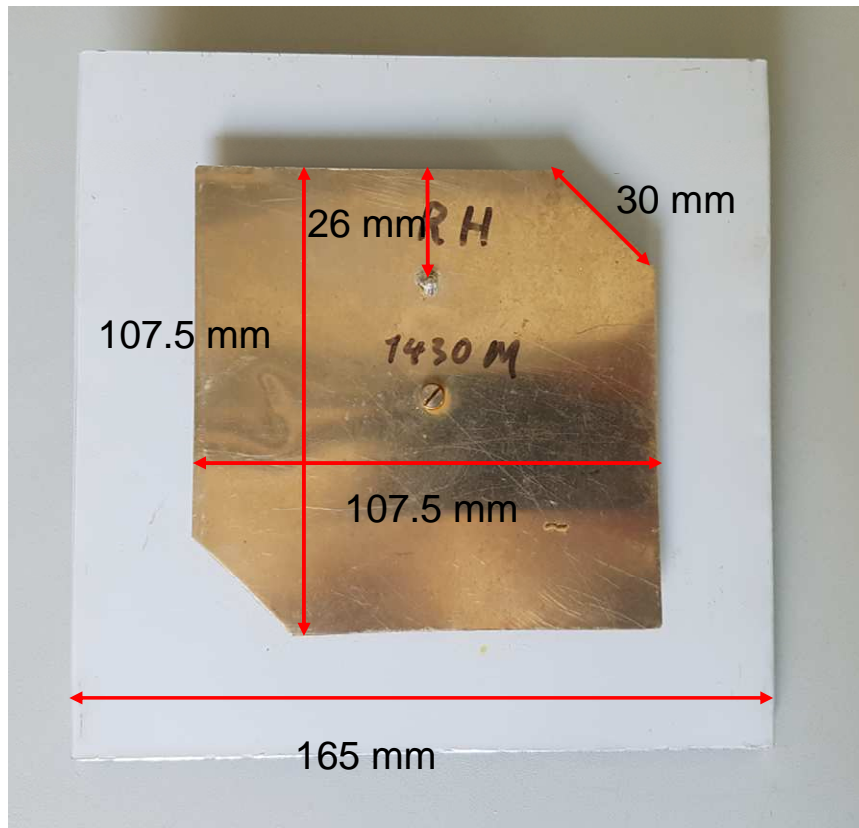

Figure 24: Air gap patch antenna top view

Two edges are cut off, which creates a circular polarization of the antenna. Without these cut-offs the polarization would be linear.

A hole is made in the reflector at the position of the feed point so that an N-connector can be fitted and the centre conductor can be connected to the radiator as shown in Fig. 25.
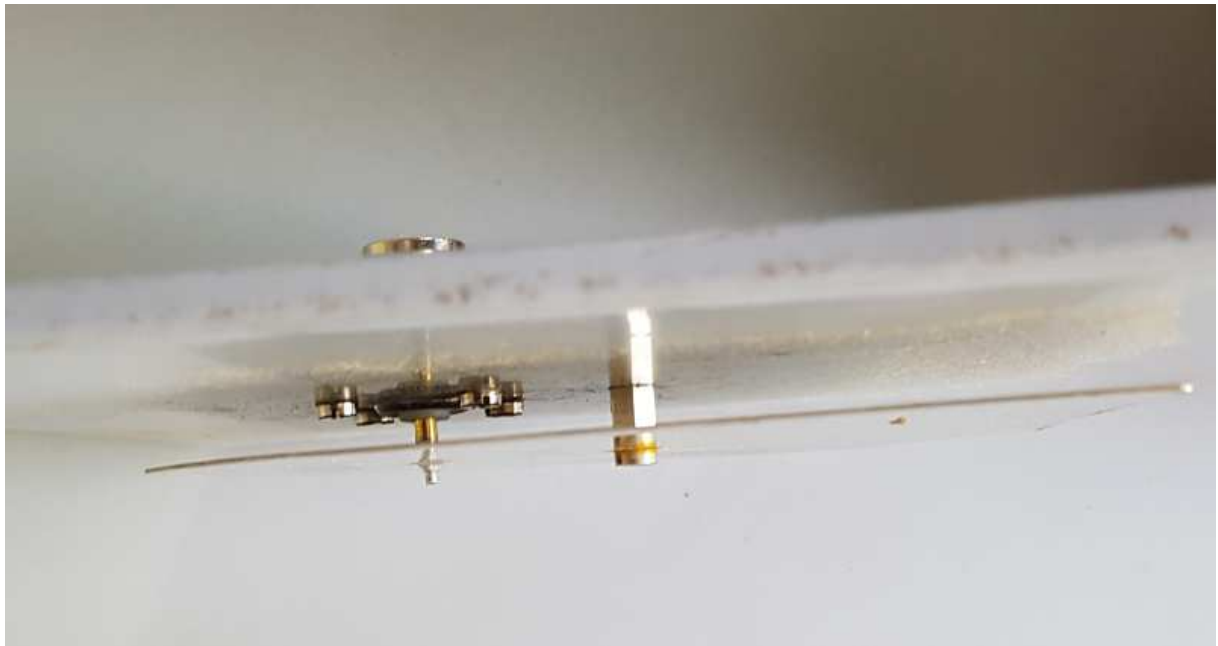
Figure 25: Air gap patch antenna side view

7.8.2. Characteristics

As can be seen from fig. 26 the design is a bit off resonance with the chosen dimensions. Probably making the radiator a bit smaller would rectify the issue.
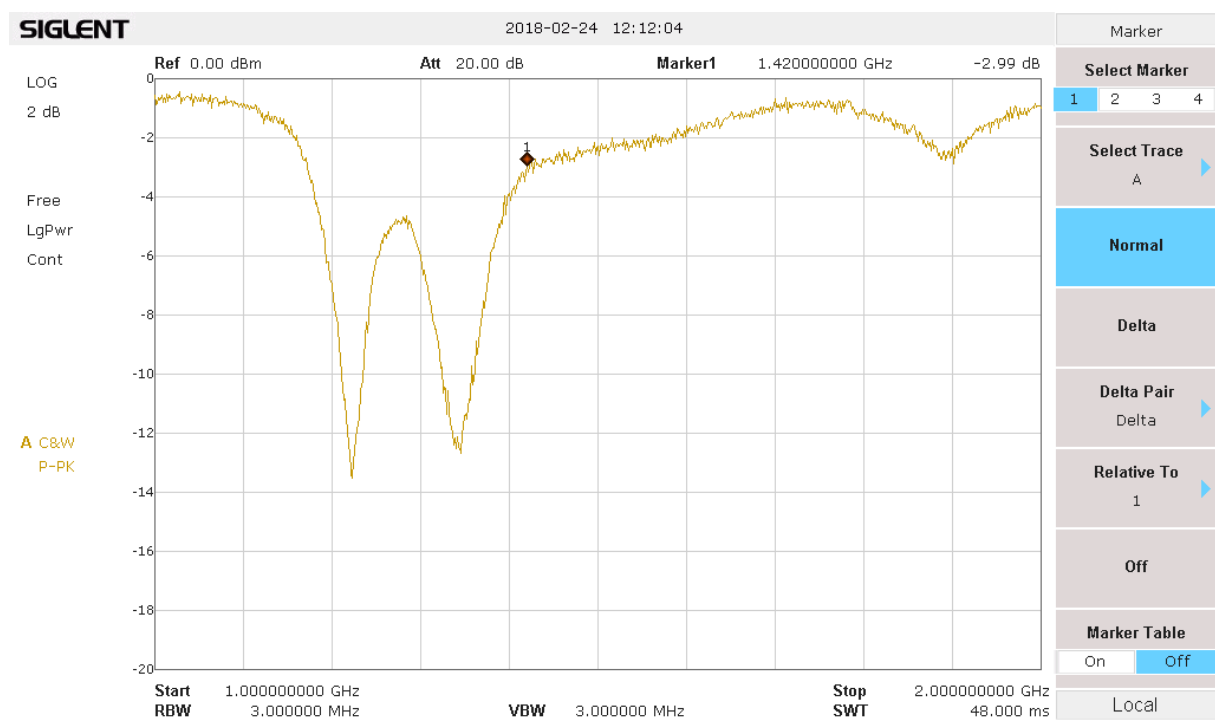

Figure 26: Air gap patch antenna return loss

The antenna pattern was measured in one orientation only. We do not expect a difference between the two orientations as the design is symmetrical and circularly polarized (fig. 27).
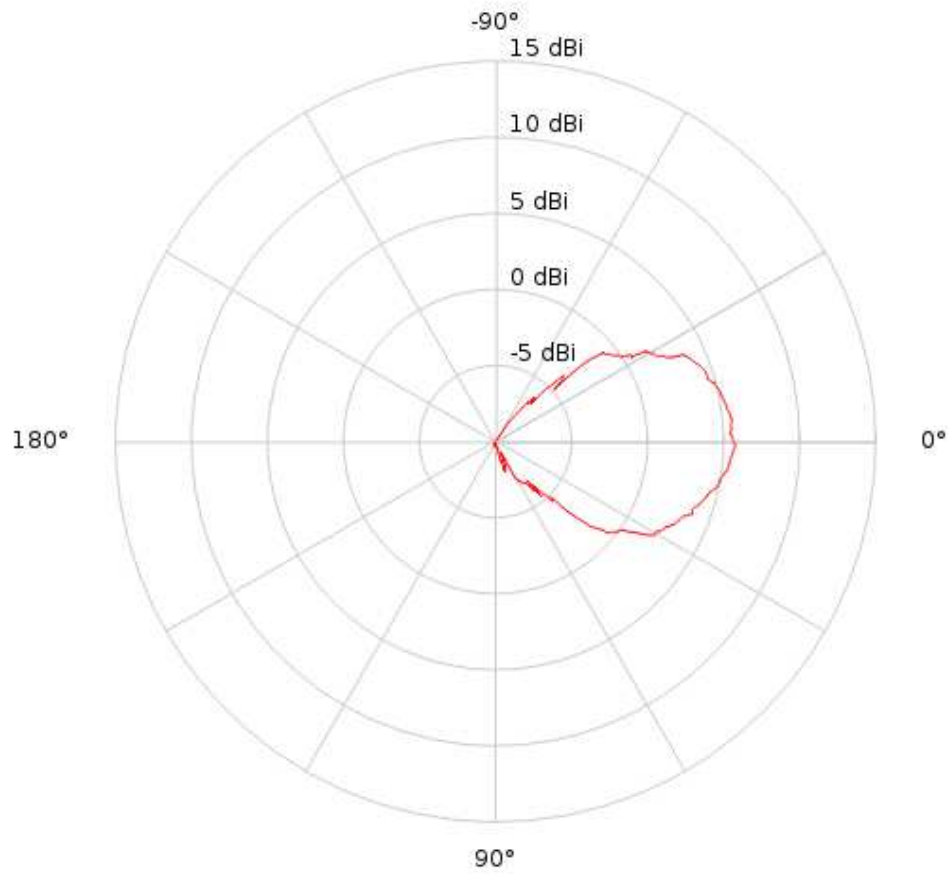

Figure 27: Air gap patch antenna pattern

Patch Yagi
7.8.3. Design
This is an interesting design made be Johannes Falk (DC5GY) [14]. It is essentially a circular patch antenna with a circular reflector and 5 evenly spaced circular directors (fig. 28).
He quotes a gain of about 12dBi with a 3 dB opening angle of 45°.
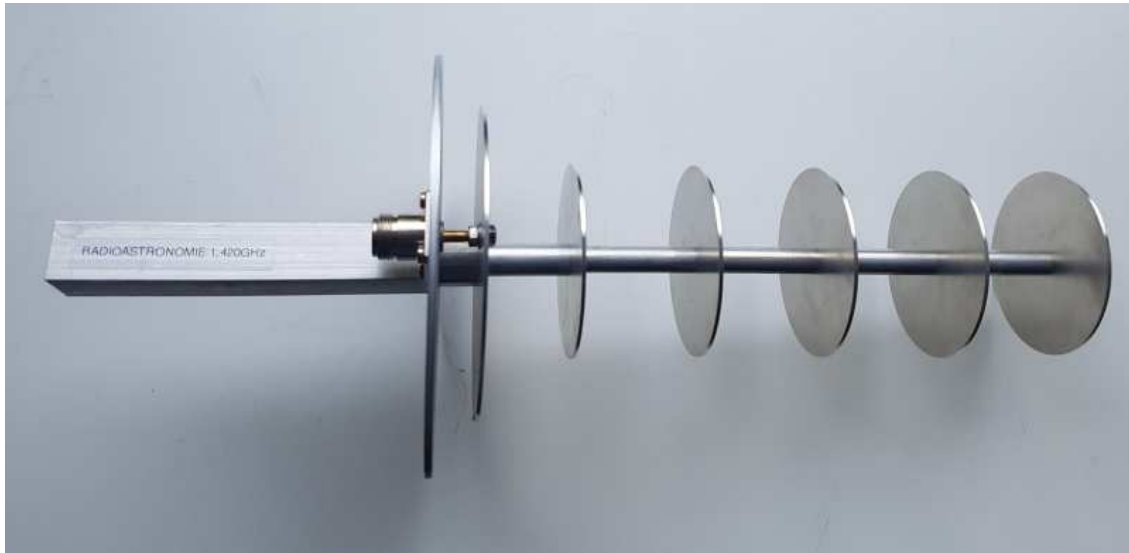

Figure 28: Patch Yagi

7.8.4. Characteristics
The resonance seems to be spot on for 1420 MHz as demonstrated by the return loss measurement shown in fig. 29.
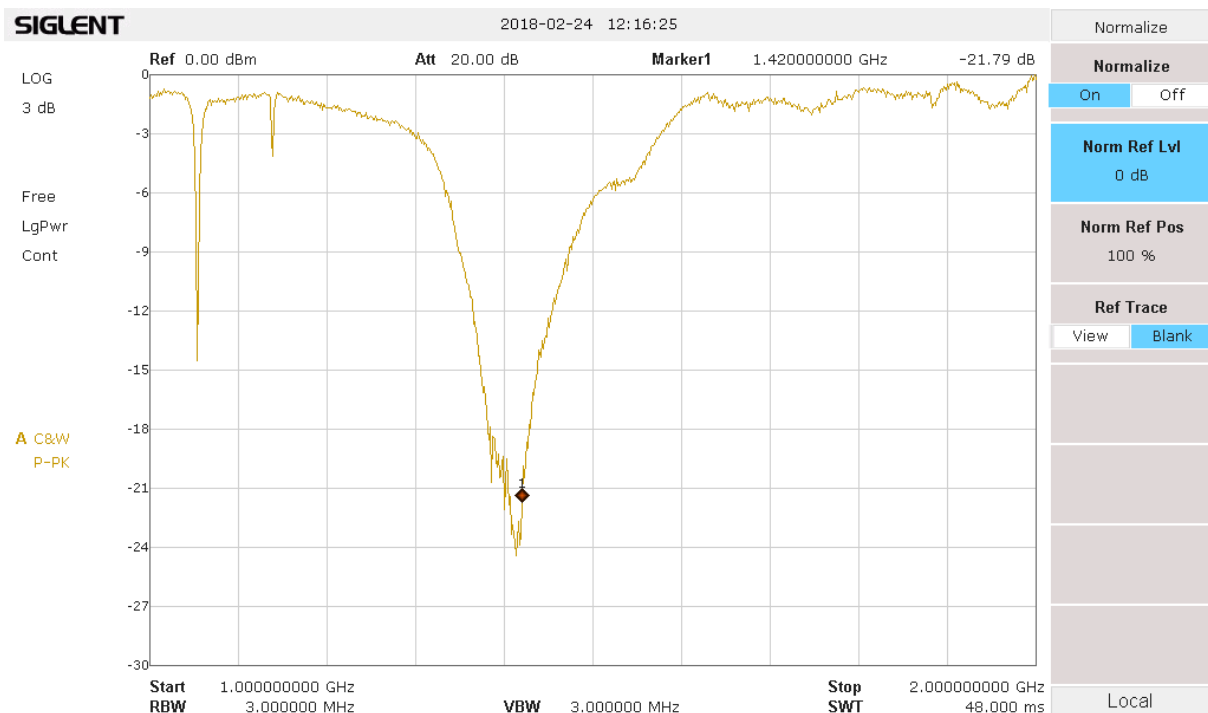

Figure 29: Patch Yagi return loss measurement

The actual measurement of the antenna (fig. 30) confirms the opening angle (beam widht) quoted. Given our uncertainty in the calibration of absolute gain measurements also the quoted gain seems to be as expected.
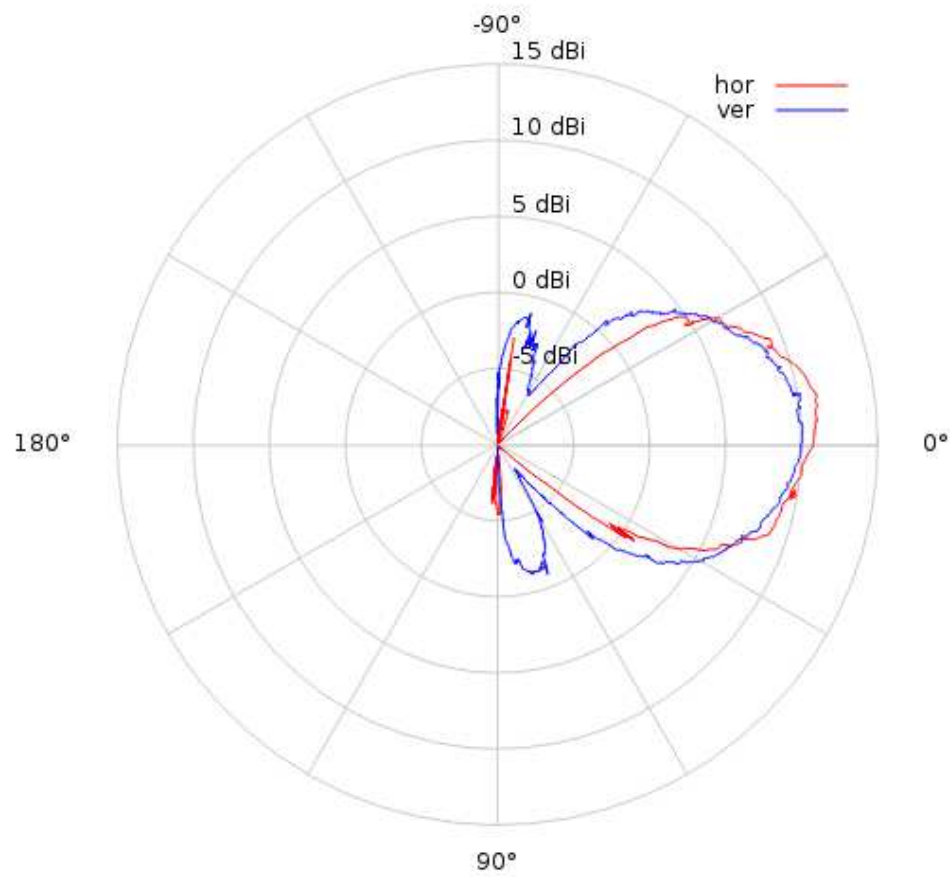

Figure 30: Patch Yagi antenna beam pattern

7.9. Rectangular horn with waveguide
7.9.1.   Design
This is a rectangular horn which ends in a rectangular waveguide with a probe (fig. 31). The rectangular waveguide is very similar to the one described in 7.6.
The opening of the horn is 438 x 309 mm.

Figure 31: Rectangular horn

7.9.2. Characteristics

As one can expect this horn is fairly wide band with good return loss over a wide frequency range (fig. 32):

Figure 32: Rectangular horn return loss measurement

7.10. 3D corner antenna
7.10.1. Design
We have used the design of a "shortened 3D corner antenna" as described by Dragoslav Dobričić. His description can be found at [15]. The dimensions were modified to adapt to 1420 MHz, the length of the side of the cube is 60 cm. The construction uses standard galvanized steel profiles from a hardware shop, cut to length. The reflecting surfaces were made from aluminium mesh, see fig. 33.

Figure 33: 3D corner antenna

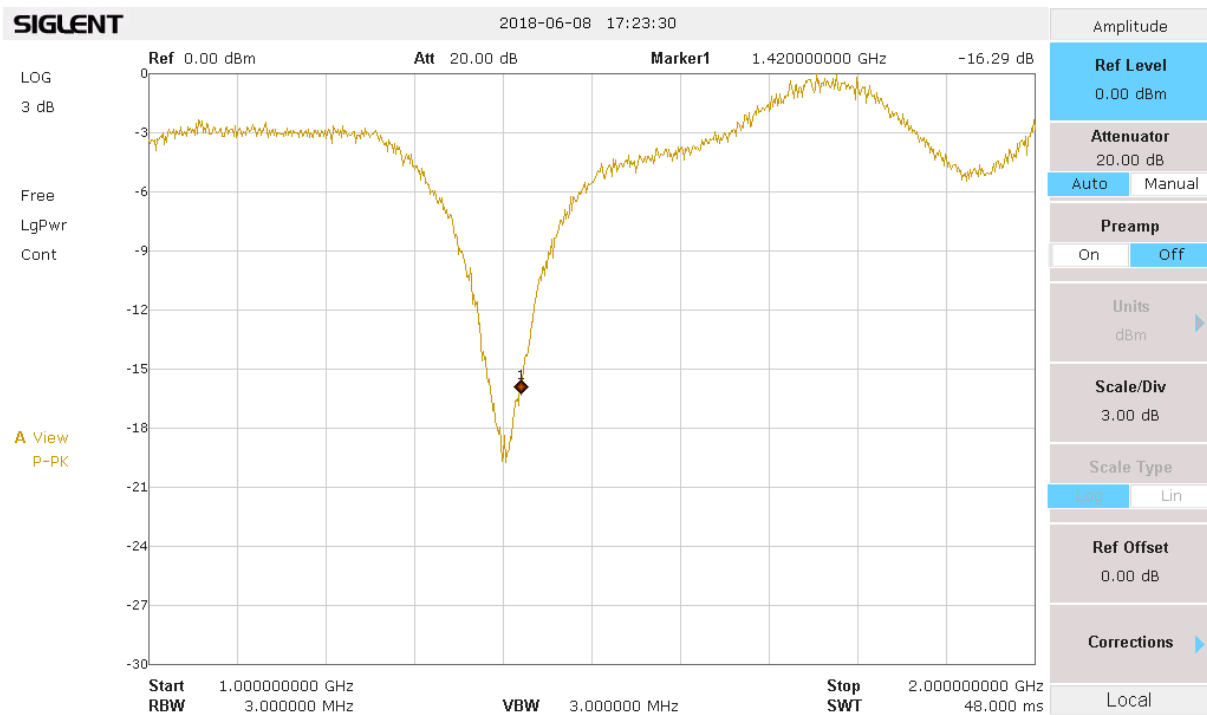## 7.10.2.   Characteristics

Figure 34: 3D corner antenna return loss measurement

The return loss of this antenna is quite reasonable with about 16 dB, and the resonance is relatively sharp (fig. 34).

7.11. SETI Horn of Plenty
7.11.1. Design
A frequently used design for the reception of hydrogen is the "SETI Horn of Plenty", described by Paul Shush in [16]. Our version was constructed from profiles and aluminium mesh similar to what has been used for the 3D corner antenna (fig. 35).

Figure 35: Horn of Plenty Antenna

It turned out that the use of this material was less than optimal. The large areas spanned by the aluminium mesh resulted in waviness of the surface. Also, the rear part is not adhering good enough to the design dimensions. All this may lead to a less than optimal performance, and using stiffer materials will most likely bring better results.
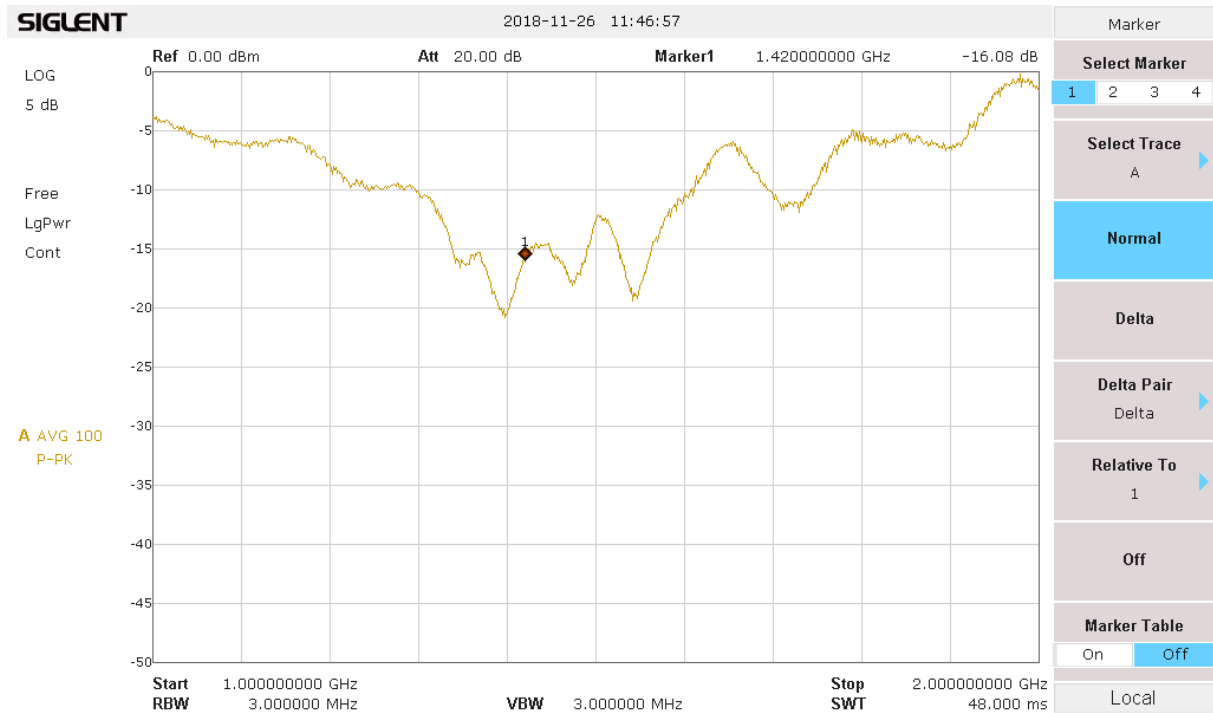
Figure 36: Return loss of horn of plenty antenna

The return loss at 1420 MHz is 16 dB, similar to what is achieved with the corner cube antenna. It is fairly "wavy" which may be due to the inaccuracies described above.

7.12. 60 cm dish (stationary) with dipole feed (aka Micro Arecibo)

Probably the most frequently used design for receiving the hydrogen emission
is a parabolic dish. Here we use a fairly small dish with 60 cm diameter. The feed is
the dipole with reflector which is described under 7.3.
The dish was used just stationary and looking straight up. This is why we have
dubbed it "Micro Arecibo" (fig. 37).

Figure 37: 60 cm dish

7.13. 90 cm dish (stationary) with dipole feed (aka Mini Arecibo)

The next step up in aperture is a 90 cm dish, hence called "Mini Arecibo". The same feed was used. Also this dish was looking straight up for observing (fig 38).

Figure 38: 90 cm dish

7.14. 3 m dish (fully steerable) with Kumar feed

Finally, the most advanced antenna and used as a reference for all testing, is a 3 m dish. This dish is mounted on an Alt/Az rotor and is fully computer controlled, shown in fig. 39. The dish has a f/D ratio of 0.3.

Figure 39: 90 cm dish

The feed is a Kumar type feed, i.e. a circular waveguide with a choke ring.
The full details of the design will be published in a different upcoming article in the SARA journal.

7.15. Other antenna options (not tested)

Of course the antennas presented here are not the only ones one can think of. Some obvious ones are missing:

- Yagi antenna
  We did build a simple Yagi. However, we found it performing much poorer than expected. We believe we must have made an error building it. Eventually we will revisit this option
- Helical antenna
  We also built one of these without much success. Helical antennas tend to be a bit critical in adhering to the calculated dimensions and in proper coupling.

Further options would include a quadfilar helix, log-periodic antennas, discones and probably quite a few more.
However we expect that such other antennas will be more difficult to build without giving any extra advantage for the reception of the hydrogen signal.

8. Why can we expect successful observations of hydrogen with small antennas?

Obviously, all these antennas differ to a large extent in their receiving area which means they have substantially different gains. The extremes are the 3 m dish on the "big" side and the dipole on the "small" side. One can expect a gain of about 30 dBi from the 3 m dish, assuming a aperture efficiency of 50%. In contrast to this, a simple dipole has a gain of just 2.5 dBi which means that there is a factor of about 560 between these two.
In this article we have claimed that hydrogen observations were possible with all the antennas presented. Of course this claim will be proven to be true in later parts of this series of articles. How can one expect to receive something with small gain antennas?

The answer to this question lies in the distribution of hydrogen.
Unlike compact objects such as stars or radio objects like supernova remnants, distant galaxies and others, hydrogen is distributed over a large area of the sky. This has a significant impact on the observation possibilities.
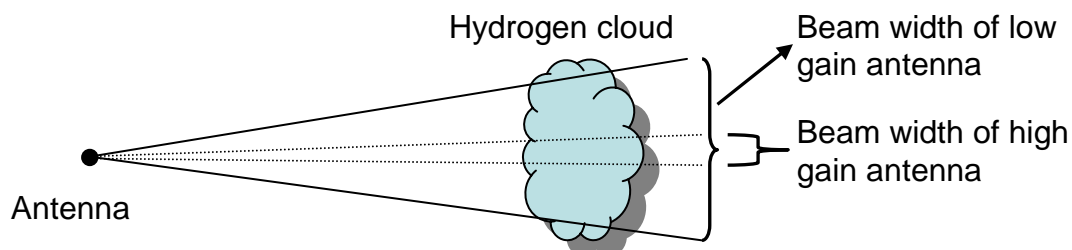

Figure 40: Geometry of antennas with different gain

Since a lower gain antenna has a wider beam compared to a higher gain antenna (fig. 40), this lower gain antenna observes more hydrogen. In fact, if the brightness of the hydrogen cloud would be constant over the complete area, the gain of the

antenna would not matter at all: Let us take two parabolic dishes with diameters d_1 and d_2 as example.

The received power falling onto the dish from an area of the sky will increase with the square root of the dish diameter, so the ratio between the two dishes will be:

$$d_1^2 / d_2^2 \qquad\qquad\qquad\qquad (1)$$

On the other hand, the beam width increases with one over the diameter squared, hence more of the sky contribute to the received power. This yields for the received power from the respective sky per unit area of the telescopes:

$$d_2^2 / d_1^2 \qquad\qquad\qquad\qquad (2)$$

Multiplying (1) and (2) obviously is = 1, independent on the respective diameters. In other words, if the brightness of a hydrogen cloud is uniform over the area observed by both telescopes, the size of the dishes does not matter for the signal intensity!

Why would one go for larger telescopes then at all? First, the brightness is not uniform over the complete sky. So if the beam width gets too large, darker parts of the sky get into the beam reducing the overall signal. The even more important thing is spatial resolution. As the beam gets larger, finer structures can no longer be resolved.

But the basic principle holds: Small antennas with correspondingly wide beams will produce an astonishingly large hydrogen signal.

It has to be noted that this principle does not hold for compact objects where the brightness is concentrated in a small spot on the sky. Nothing is gained here by widening the beam.

9. The "Hydrogen Team"
Quite a few people from the Astropeiler Stockert team have enjoyed the fun of designing and building antennas, measuring them and doing other measurements and observations. So this has been very much a team effort. Thomas Buchsteiner, Elke Fischer, Hans-Peter Löge, Frank Tägl, Horst Thum and some others have contributed to this work.

References:
[1] H.C. v.d. Hulst, Ned.Tijd.Natuurkunde, vol.11, p210 (1945)
[2] http://hyperphysics.phy-astr.gsu.edu/hbase/quantum/h21.html
[3] H.I. Ewen and E.M. Purcell, Nature vol.168, p.356 (1951)
[4] C.A. Muller and J. H. Oort, Nature vol. 168, p.357 (1951)
[5] http://www.nrao.edu/archives/Ewen/ewen_HI.shtml
[6] http://www.nrao.edu/whatisra/images/docmin.jpg
[7] HI4PI Collaboration, A&A 594, A116 (2016)
[8] http://cdsarc.u-strasbg.fr/viz-bin/qcat?J/A+A/594/A116
[9] https://astro.uni-bonn.de/~bwinkel/research.html

[10] J.H. Oort, F.T. Kerr and G. Westerhout, MNRAS 4, 379 (1958)

[11] https://www.youtube.com/watch?time_continue=6&v=Q2mgpsTFuV8

[12] https://www.youtube.com/watch?v=N0Ja6jpju00

[13] http://lea.hamradio.si/~s53mv/wumca/sbfa.html

[14] http://www.falk-on-tour.de/Antennen.html

[15] blog.freifunk-mainz.de/wp-content/uploads/2013/08/Shortened-3D-Corner-Reflector-Antenna.pdf

[16] http://www.setileague.org/articles/horn.htm

About the Author: Dr. Wolfgang Herrmann is the president of the "Astropeiler Stockert e.V.", the organization which takes care of the instrument.
He received his PhD in Physics from the University of Bonn. He has spent most of his professional career in the telecommunication industry. At retirement age, he now enjoys learning as much as possible about radio astronomy, doing observations and improving the instrument.
Contact the author at messbetrieb@astropeiler.de